Simultaneous separation and detection of cations and anions on a microfluidic device with suppressed electroosmotic flow and a single injection point

Brent R. Reschke,[a] Jarrod Schiffbauer,[b] Boyd F. Edwards[b] and Aaron T. Timperman*[a]

Received 20th October 2009, Accepted 8th March 2010
First published as an Advance Article on the web 26th March 2010
DOI: 10.1039/b921914e

A rapid and simultaneous separation of cationic and anionic peptides and proteins in a glass microfluidic device that has been covalently modified with a neutral poly(ethylene glycol) (PEG) coating to minimize protein adsorption is presented. The features of the device allow samples that contain both anions and cations to be introduced from a central flow stream and separated in different channels with different outlets—all in the presence of low electroosmotic flow (EOF) imparted by the PEG coating. The analytes are electrophoretically extracted from a central hydrodynamic stream and electrophoretically separated in two different channels, in which pressure driven flow has been suppressed through the use of hydrodynamic restrictors. Having different outlets for the electrophoretic separation channels that are spatially separated from the injection enables coupling with further downstream functionalities or off-chip detection, such as mass spectrometry. A plug of charged analyte is hydrodynamically pumped to the sampling intersection and anions from the plug migrate electrophoretically toward the anode in one channel while cations migrate toward the cathode in the other channel due to suppressed EOF from the PEG coating. The separations presented here required less than a minute to complete and produced average separation efficiencies of up to about 3,500 plates from a separation length of 2 cm. The extraction efficiency of both cations and anions from the hydrodynamic stream is determined experimentally and compared with a previously reported model that was used to determine anion extraction efficiency. The extraction efficiency is determined to be 87% and 98% for the two sample mixtures analyzed, and the values predicted by the model are within 3.5% of the experimental data. It is anticipated that this basic approach for simultaneous separation of anions and cations with reduced EOF will be integrated into larger microfluidic systems because the design provides separate outlets that can feed downstream processes or linked to off-chip detection.

Introduction

Capillary electrophoresis (CE) and the analogous method, microchannel electrophoresis (ME), can provide separations with unparalleled efficiencies. ME differs from CE by the channel intersections around which solutions can be steered electrokinetically. As a result, the intersections and electrokinetic steering allow the highly efficient separations to be integrated with multiple processes such as sample preconcentration,[1–5] digestion,[6–9] and purification[6–10] as well as multidimensional separations,[11–13] in microfluidic systems. Additionally, the miniaturization and integration of these systems reduce sample and reagent consumption while having less contamination and sample loss compared to traditional methods. Lastly, miniaturization of these methods onto microfluidic platforms is beneficial because they are potentially disposable, have fast analysis times, and provide high throughput.[14]

Currently, there is a need for improved protein separations and downstream sample processing in proteomics. Proteomics, as a field, is instrumentally limited and could benefit from improved methods for the separation and identification of peptides and proteins from complex mixtures. An aim of proteomics is to characterize as many proteins as possible in a sample and determine their function in the biological system as a whole,[15] which is at best a challenging task with current technologies. A typical proteomic investigation can range from the comprehensive analysis of whole cell lysates to the analysis of protein complexes.[16–24] As a result, proteomic samples are extremely complex due to the wide dynamic range and the diverse nature of proteins in the sample. The diverse nature of proteins stems from the different functional groups associated with the various amino acids. Any particular protein will generally contain residues with hydrophobic, hydrophilic, polar, non-polar, acidic and basic functional groups. Due to the vast array of acidic and basic functional groups that can be present in a protein, a typical proteomic sample at near neutral pH will contain a mixture of positive and negative proteins. Therefore, methods to simultaneously separate cations and anions, such as CE and ME, are frequently used, although separation by these free solution methods is not without challenges.

Non-specific adsorption of proteins to the microchannel or capillary walls and difficulty in maintaining protein solubility are two considerable challenges encountered when analyzing proteins with CE or ME. To reduce non-specific adsorption to the microchannel or capillary walls, numerous coatings have

[a]*C. Eugene Bennett Department of Chemistry, West Virginia University, Morgantown, WV, 26506, USA*
[b]*Department of Physics, West Virginia University, Morgantown, WV, 26506, USA*

been developed that reduce the interaction of the proteins with the surface. Two general approaches have been developed that utilize either positive coatings and low pH or neutral coatings with pH values near or above neutral. When positive coatings are used the pH is lowered to increase the positive charge on the proteins, thereby increasing the electrostatic repulsion between the proteins and the surface.[25–29] However, lower pH values decrease the protein solubility, particularly for proteins with a molecular mass >20 kDa.[28,30,31] In addition, the use of the positive coating creates a highly charged wall that produces a large EOF, which provides simultaneous detection of anions and cations but also introduces a substantial separation bias.[32] In this case, with anodic EOF, the separation bias reduces the separation time for the anions, which must elute before the neutral marker, and increases the separation time for the cations that elute after the neutral marker.

Another common approach is to use neutral hydrophilic coatings at pH values ≥7. Many coatings have been used, but those made from PEG and poly(ethylene oxide) (PEO) have been shown to have excellent resistance to interactions with proteins.[33–38] Often these coatings are made permanent through covalent modification, which also provides an additional advantage in that they do not interfere with detection strategies, like mass spectrometry (MS), that are routinely used for protein and peptide identification and sequencing.[34] While these coatings are excellent at resisting protein adsorption, they also concomitantly minimize the magnitude of the EOF to levels below the electrophoretic mobility of most analytes. Thus, the simultaneous separation of anions and cations using standard CE or ME formats is prevented.

To enable the use of capillaries with suppressed EOF while maintaining the ability to simultaneously analyze both cations and anions, a clever approach called dual-opposite injection capillary electrophoresis (DOI-CE) was developed.[32,39–48] To perform a separation with DOI the cations are injected at the anodic reservoir and the anions are injected at the cathodic reservoir. When an electric field is applied across the capillary, the cations and anions migrate toward each other after being injected at opposite ends of the capillary. Typically the analytes are detected at a single point that is generally in the middle of the capillary. This technique can remove the separation bias associated with traditional CE separations.[32] However, the possibility exists for co-detection of positive and negative analytes if they pass the detection point at the same time. Placement of the detector can be optimized to minimize co-detection, but it requires multiple runs, making it impractical for applications in which sample is limited or many unknowns are analyzed. In addition, simultaneous injection with DOI requires two sample vials and twice as much sample. Furthermore, DOI-CE using traditional equipment is difficult to interface with other techniques, like liquid chromatography (LC) or MS, because each sample is injected and elutes through both ends of the capillary.[32]

Previously, the utility of DOI on a microfluidic chip was reported by Wang *et al.*[49] The results of this work demonstrated a rapid and simultaneous separation of anions and cations on a poly(methyl methacrylate) (PMMA) chip with low EOF. The design of the system was similar to DOI-CE in that the sample was injected into both ends of the microchannel and the anions and cations migrated toward each other for detection near the middle of the microchannel. However, the design used in this work would be difficult to interface with other techniques and the possibility of co-detection still exists.

Presented in this paper is a microfluidic device that electrophoretically extracts ions from a single hydrodynamic sample stream and simultaneously separates and detects cations and anions in two opposing electrophoretic channels, making this design well suited for applications such as 2D LC-CE separations and process monitoring. Furthermore, because the analytes are separated in two different channels it is possible to collect the separated cations and anions without recombination, and subject them to further downstream processing or off chip analysis, such as MS. The device design enables sample injection from a hydrodynamic flow stream while still achieving good separation efficiencies through the use of hydrodynamic restrictors (HDRs) at the entrance to the electrophoretic separation channels. Additionally, neutral PEG coatings also minimize bulk flow in the electrophoretic separation channels so electrophoresis is the dominant force for mass transport. The sample, a mixture of a cation and anions, is electrokinetically introduced into a double-tee injector and then hydrodynamically injected by pumping the sample plug to a sampling intersection using pressure driven flow. As the sample plug passes through the intersection the ions are electrophoretically extracted and cations migrate toward the cathode and anions migrate toward the anode in two opposing channels with separate outlets that are not associated with the double-tee injector (see Fig. 1). Extraction of the anions and cations into their respective separation channels and adequate suppression of the pressure driven flow and EOF in the electrophoretic separation channels are demonstrated. As commonly achieved with ME, the separations are fast (<1 min) and the separation efficiencies for the fluorescent dyes, proteins and peptides, are good (~200 to 3000 plates). This technique also shows the ability to effectively remove the separation bias observed in traditional CE separations by

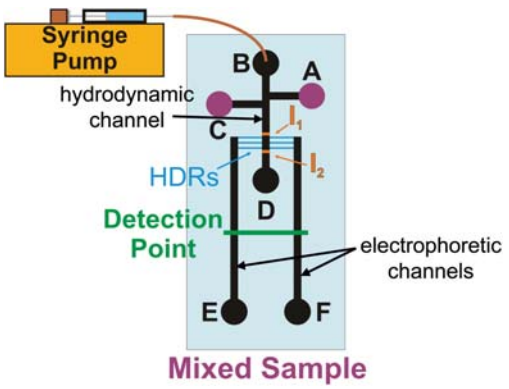

Fig. 1 A schematic of the microfluidic device is shown. Sample is loaded into reservoirs A and C. A sample plug is formed at the double-tee intersection and the plug is hydrodynamically pumped past the cross-intersection with the electrophoretic channels. The hydrodynamic restrictors (HDRs), shown in blue, reduce the hydrodynamic flow to a negligible level in the electrophoretic separation channels. The orange regions labeled I_1 and I_2 are used to experimentally determine the extraction efficiency. Reservoir D serves as an outlet for the hydrodynamic flow. The electropherograms are obtained by monitoring the detection points, which are 2 cm from the sampling intersection.

providing equivalent times for the separation of anions and cations as previously reported for DOI-CE.[32,40,47] The extraction efficiency is also high and is found to be >87% for both anions and cations, and is compared with a previously reported theoretical model that was originally evaluated with an anionic tracer.[50] In summary, the simultaneous separation of anions and cations into distinct channels in a low EOF system coated to minimize non-specific adsorption is demonstrated. It is anticipated that this device will be used for applications that require downstream sample processing or off-chip analysis with MS.

Experimental

Chemicals and reagents

Unless otherwise noted all chemicals were purchased from Sigma-Aldrich (Milwaukee, WI). The running buffer used was 25 mM phosphate buffer, pH 7. The fluorescent dye mixture consisted of 5 μM rhodamine 123 (R123), 10 μM 6-[fluorescein-5(6)-carboxamido]hexanoic acid (FLCA), and 20 μM fluorescein (FL) dissolved in the running buffer. Tetramethylrhodamine-5-iodoacetamide dihydroiodide (TMRIA) was purchased from Invitrogen (Carlsbad, CA). The peptide and protein mixture consisted of 30 μM fluorescein isothiocyanate (FITC) labeled albumin from bovine serum, 70 μM FITC labeled casein from bovine milk, 15 μM FITC labeled avidin from chicken egg white, and 100 μM TMRIA labeled Ac-D-Arg-[Cys-Met-Leu-Asn-Arg-Val-Tyr-Arg-Pro-Cys]-NH_2 (Peptides International, Louisville, KY). The peptide was labeled in house using the protocol provided by Invitrogen and purified using C_{18} SpinTips (Protea Biosciences Inc., Morgantown, WV). *N*-(Triethoxysilylpropyl)-*O*-poly-(ethylene oxide) urethane (M_w 4000–5000 g/mole) for the PEG coating solution was purchased from Gelest (Morrisville, PA). Deionized water was obtained from a Barnstead International NanoPure Infinity (Dubuque, IA) that dispenses water with a nominal resistivity of 18.3 MΩ cm.

Device fabrication

A schematic diagram of the microfluidic device used in this work is shown in Fig. 1. Soda lime glass wafers coated with a layer of photoresist and a layer of chromium were purchased from Telic Co. (Valencia, CA). The glass microfluidic device was fabricated using standard photolithography and wet chemical etching techniques.[51,52] The etched trapezoidal microchannels had a top width, bottom width, and depth of 100 μm, 50 μm, and 20 μm, respectively. The HDRs were made using a MP-100-UV micromachining system (Oxford Lasers, Oxon UK).[51] This micromachining system utilizes a frequency doubled copper vapor laser with emission at 255 nm for ablation. The laser ablation process created 10 parallel channels with dimensions of 5 μm wide by 40 μm deep and 10 μm spacing between each channel. The PEG coating solution, which is used to minimize the adsorption of proteins to the glass surface, was made according to previous methods.[34] Briefly, 20 mg of the *N*-(triethoxysilylpropyl)-*O*-poly-(ethylene oxide) urethane was dissolved in 10 mL of extra dry toluene with 10 μL of triethylamine. The solution was then pumped onto the microfluidic device at a flow rate of 1 μL min^{-1} for about 2 hours. Next, the PEG solution was removed from the channels with helium from a pressure vessel at 100 psi. Lastly, the device was cured in an oven overnight at 60 °C.

Microfluidic control and imaging

The microfluidic device was imaged with an Olympus IX 81 epifluorescence microscope (Center Valley, PA) with a Hamamatsu EM-CCD digital camera (model C9100-12, Bridgewater, NJ). Detection of the analytes in both channels is achieved with a single detector. A microscope with an epifluorescence system allows both channels, which are separated by about 1.3 mm, to be monitored simultaneously. While only one detector is needed, the limits of detections (LODs) are somewhat sacrificed, as the optical system, particularly the 10× objective with a numerical aperture of 0.3, reduces the signal to noise ratio (*S*/*N*). Slidebook v 4.1 (Denver, CO) was used to analyze the collected data. In addition, collected images were flat field corrected and background subtracted using the Slidebook software. Voltages were controlled using a six electrode power supply that was built in-house using an EMCO Octo-channel High Voltage System (Sutter Creek, CA). The sample plug was hydrodynamically injected using a Kd Scientific syringe pump (model 7803118, Holliston, MA). Fused silica capillary (100 μm ID, 360 μm OD) purchased from Polymicro Technologies (Phoenix, AZ) was used to connect the microfluidic device to a 25 μL syringe (1700 Series Hamilton, Reno, NV).

Characterization of EOF

The magnitude of the EOF was first determined on an uncoated microfluidic device by calculating the mobility of rhodamine B, a neutral marker, similar to a procedure used in our previous work[50] and found to be 3.42×10^{-4} cm^2 V^{-1} s^{-1}. To determine the degree of suppression of EOF the surface was coated with PEG and the experiment was repeated. After coating, the mobility of rhodamine B was found to be 2.48×10^{-5} cm^2 V^{-1} s^{-1}, corresponding to a 92.8% suppression in EOF. Therefore, electrophoresis is the dominant mode of transport in the electrophoretic side channels because of the suppressed of EOF.

Sample introduction, injection and extraction on the microfluidic device

Simultaneous separation and detection of both cations and anions are achieved with four distinct processes: (1) the analyte is electrophoretically introduced into a double-tee injector in the hydrodynamic main channel (Fig. 2a), (2) the sample plug is hydrodynamically injected and pumped toward the sampling intersection (Fig. 2b), (3) the cations and anions are electrophoretically extracted into the two opposing separation channels (Fig. 2c), and (4) the analyte ions are separated and detected in the electrophoretic channels (Fig. 2d).

Sample introduction into the hydrodynamic channel is accomplished using the following procedure as shown in Fig. 2. The sample mixture was first placed in reservoirs A and C (Fig. 1). A voltage of +3000 V was applied to electrode A while electrode C was held at ground (Fig. 2a). The application of the voltage caused the anions and cations to cross-migrate and fill the double-tee injector due to suppressed EOF. During sample introduction, electrodes E and F were floating and the syringe

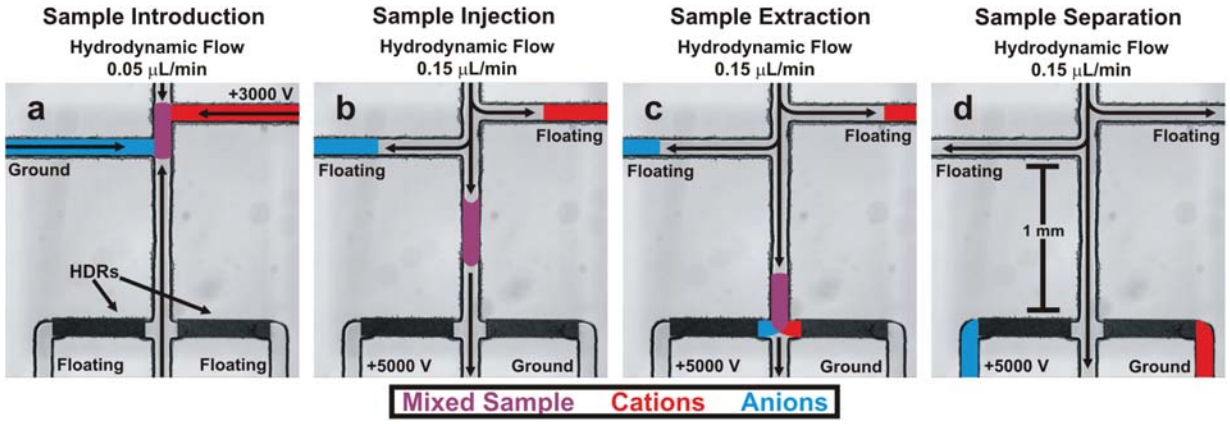

Fig. 2 The stages of the sample injection and separation are shown with an illustration superimposed on a optical micrograph of the device. The entire device is coated with a neutral PEG coating that reduces protein adsorption and EOF. (a) A sample plug is formed in the hydrodynamic channel as cations and anions migrate electrophoretically from opposite sample reservoirs. Buffer is pumped from both reservoirs B and D to hydrodynamically pinch the sample plug. (b) The voltages are switched and the hydrodynamic flow is increased to inject the sample plug toward the sampling intersection. (c) As the sample plug enters the sampling intersection the cations and anions migrate according to their electrophoretic mobility and are extracted into opposite channels. (d) The separation of the anions and cations begins as they migrate through their respective electrophoretic channels.

pump is set to a flow rate of 0.05 μL min^{-1}. Sample was hydrodynamically "pinched" in the double-tee injector using the syringe pump and excess buffer in reservoir D, approximately 200 μL compared to about 100 μL in all other buffer reservoirs.

To inject the sample plug (Fig. 2b), the syringe pump flow rate is increased to 0.15 μL min^{-1}, electrodes A and C were switched to float, a voltage of +5000 V was applied to electrode E, and electrode F was held at ground. These voltages correspond to an electric field of about 400 V cm^{-1} over the separation channels. The increased flow rate at the syringe pump causes the sample plug to be hydrodynamically pumped toward the sampling intersection and the remaining analyte in channels A and C to be pushed away from the double-tee injector to help define the sample plug. As the sample plug enters and passes through the intersection the anions and cations are extracted into the two opposing separation channels (Fig. 2c), where the separation of the anions and cations in the two opposing channels begins (Fig. 2d). Finally, the anions and cations are detected with a single CCD camera that images each channel at the two detection points, a common distance from the sampling intersection as shown in Fig. 1.

When the flow rate is increased to 0.15 μL min^{-1} and the voltages are switched, the image collection with the CCD is started using the Slidebook imaging software. Electropherograms were acquired using a 10× objective while imaging both channels simultaneously at the detection point at a distance of 2 cm from the sampling intersection. The images in the stream acquisition were captured using a 100 ms exposure time with 2 × 2 binning of the CCD. Regions (88 μm × 10 μm) on the acquired images were created with the Slidebook software at the detection point in each channel to extract the intensity *vs.* time data, which were used to generate the electropherograms.

CE separations

For comparison purposes, separations of all samples were repeated using a Beckman-Coulter P/ACE MDQ Capillary Electrophoresis System (Fullerton, CA). Two sets of experiments were performed, one set on a bare fused silica capillary 50 μm ID × 360 μm OD × 31 cm, with detection at 21 cm. The 50 μm ID capillary was used because its cross-sectional area is nearly equivalent to the cross-sectional area of the microchannels used. The other set of experiments was performed on a PEG coated capillary of the same dimensions. The UV photodiode array (PDA) detector was used for the peptide and protein mixture with the reported electropherograms recorded at 214 nm. The laser induced fluorescence (LIF) detector was used for the fluorescent dye mixture with 488 nm excitation and 520 nm emission. In addition, the experiments were designed such that the electric field and plug length used for the CE separations were the same as the parameters used in the microfluidic experiments.

Determination of the extraction efficiency

The extraction efficiency (η) or the degree of extraction of ions from the hydrodynamic stream was determined using a procedure similar to our previous work.[50] The extraction efficiency is defined as the fraction of sample that migrates into the electrophoretic channel and is removed from the hydrodynamic flow stream. The experimental extraction efficiency was determined from the summed intensities within the orange boxes I_2 and I_1, shown in Fig. 1, and calculated using the equation $\eta = 1 - I_2/I_1$. These experimentally derived values were then compared with the theoretically predicted values using the empirical solution with a channel aspect ratio of ∞; similar to our previous work.[50]

Results and discussion

Device design

Presented herein is a microfluidic device for rapid, simultaneous electrophoretic separation of a mixture of cationic and anionic proteins, peptides, and dye molecules with suppressed EOF. The design and function of the microfluidic device share many characteristics with DOI-CE with two noteworthy differences:

(1) anions and cations are separated in different channels with separate outlets, and (2) the sample is extracted from one central sample stream that is pumped hydrodynamically.

In this system, the entire device is coated with a neutral coating that reduces adsorption and concomitantly EOF. Therefore, a typical electrokinetic injection scheme[53–61] cannot be used for injection of both anions and cations, and an alternate scheme is needed. A number of different injection schemes can be used, including electrophoretic injection from two reservoirs or flow gating[62–67] used by Jorgenson and others.

Because of the reduced EOF, the cations and anions migrate into opposite directions in the microchannels. Therefore, injection of a sample plug that contains both cations and anions is accomplished by first electrophoretically introducing the analytes into a double-tee injector from opposing reservoirs (Fig. 1 and 2a). After formation of the sample band in the central injection channel the analytes are hydrodynamically pumped to the sampling intersection as shown in Fig. 2b. As the analyte plug passes through the sampling intersection, the anions and cations are electrophoretically extracted, separated and detected in opposing channels (Fig. 2c and d). Using hydrodynamic flow allows both anions and cations to be pumped to the sampling intersection in a single flow stream without an electrophoretic bias. In fact, at low hydrodynamic injection flow rates the injection bias can be completely removed because 100% extraction efficiency is possible with the device design.[50]

Although use of the pressure driven flow for sample injection has several advantages, it is important to minimize its deleterious effects on the electrophoretic separation. An important consideration is the hydrodynamic flow through the electrophoretic channels must be suppressed to minimize Taylor dispersion. If Taylor dispersion is significant, it can substantially increase band broadening and reduce the separation efficiency. Suppression of the bulk hydrodynamic flow that can degrade the electrophoretic separation is accomplished with a series of parallel, high aspect ratio channels. These channels are termed HDRs[51] and restrict the linear hydrodynamic velocity as a function of the width squared.[68]

Because of the unique design of the sampling intersection it is possible that hydrodynamic flow through the electrophoresis channel could add significant broadening if the HDRs do not sufficiently suppress the hydrodynamic flow. To investigate whether the hydrodynamic flow in the sample injection affects migration through the electrophoretic channels, the hydrodynamic flow rate through the central sample introduction channel was increased from 0.15 μL min^{-1} to 0.50 μL min^{-1} as shown in Fig. 3. The data shows that the migration time of FLCA does not vary significantly as the average values for each flow rate are within one standard deviation ($n = 5$) of the migration time at 0.15 μL min^{-1}, the experimental flow rate. Furthermore, if an effect was to be observed, the migration time of the FLCA should decrease as the flow rate is increased and this trend is not observed. Therefore, the HDRs suppress the hydrodynamic flow in the electrophoretic side channels to a negligible amount for this flow range and consequently the migration time is independent of the hydrodynamic flow rate through the main injection channel. As a result, the contribution to flow from the hydrodynamic pressure is negligible at 0.15 μL min^{-1}.

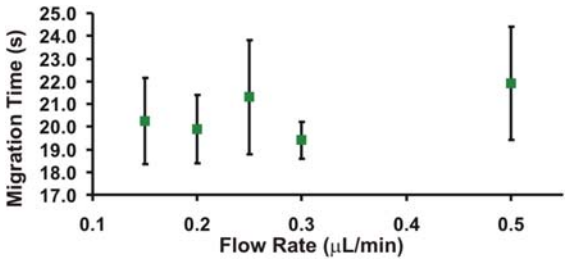

Fig. 3 Injection flow rate *vs.* migration time. The migration time of FLCA through the anionic electrophoretic channel is shown as a function of the hydrodynamic flow rate in the sample introduction channel (which connects reservoirs B and D). The data indicate that there is no discernible decrease in the migration time as the hydrodynamic flow rate is increased from 0.15 μL min^{-1} to 0.50 μL min^{-1}. Therefore, the HDRs reduce the hydrodynamic flow to a negligible level in the electrophoretic channels.

Additionally, the PEG coatings that reduce surface adsorption also reduce EOF. Consequently the device is designed to work well with very low EOF, and relies on low EOF for electrophoretic injection of the anions and cations into opposing channels. If bulk flow is present, it will cause anions to be injected into the cation separation channel (channel F) and cations to be injected into the anion separation channel (channel E). Also the low EOF allows both the anions and the cations to receive near equivalent separation times, improving the resolution of the cations as previously reported for DOI-CE.[32,40,47]

Another consideration is the amount of sample extracted from the hydrodynamic flow stream into the electrophoretic separation should be high. High extraction efficiency ensures the amount of sample lost is low and the limits of detection are not increased significantly. As a result, the hydrodynamic flow rate used to inject the sample plug is critical. It must be fast enough to prevent excessive longitudinal diffusion of the sample plug and keep the injection time relatively short, but not so fast that most of the analyte is washed through the sampling intersection resulting in low extraction efficiency.

Finally, although not demonstrated here, the two separation channels with distinct sample inlets and outlets facilitate coupling with off-column detection such as MS or further downstream sample processing. This capability is not shared by DOI-CE and devices with similar designs in which both ends of the capillary or microchannel are used simultaneously as inlets and outlets. In other designs both ends of the capillary or microchannel serve as inlets; therefore direct, physical attachment to the ESI emitter or further downstream sample processing is precluded.

Study of band broadening

Ideally, the injection and extraction sequence should introduce narrow bands into the separation channels and not contribute significantly to band broadening. To further evaluate the performance of the microfluidic device, the amount of band broadening from the different features of the design is investigated. The contribution to broadening from the sample injection and hydrodynamic flow, HDRs and the turns in the separation

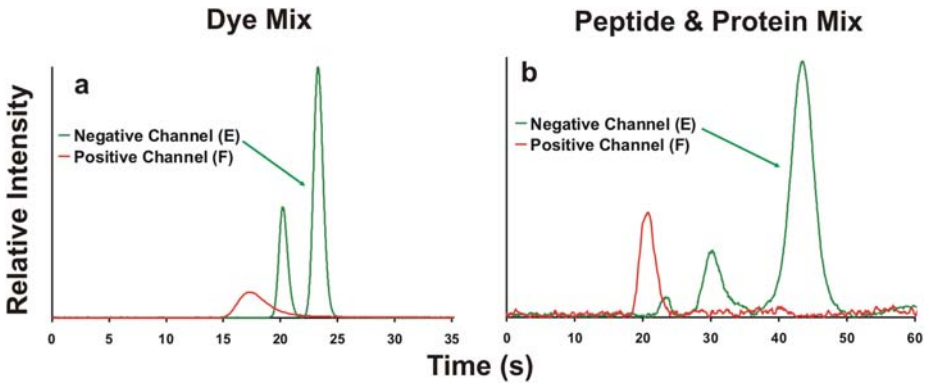

Fig. 4 Representative electropherograms of the separations performed on the PEG coated (low EOF) microfluidic device. Sample injection from a central channel is achieved, and anions and cations are separated in different channels. An electropherogram of the fluorescent dye mixture is shown in (a), and an electropherogram of the protein and peptide mixture is shown in (b). Each component was baseline resolved with high efficiencies in <1 minute.

channel, and the separation channel itself is determined by measuring the peak width at half-height ($w_{½}$) at various locations along the analyte path. First, the $w_{½}$ immediately after injection is measured and found to be 1.00 s. Second, immediately before the electrophoretic extraction the $w_{½}$ is measured to be 1.39 s. Third, $w_{½}$ after extraction into the electrophoretic channels through the HDRs and turns is 1.51 s. Fourth, the $w_{½}$ at the detection point is measured to be 3.15 s.

The various sources of band broadening contribute to the total variance as a sum of the variances: $\sigma^2_{Total} = \sigma^2_{injection} + \sigma^2_{HDRs\&Turns} + \sigma^2_{Channel}$.[69] From this equation and the peak widths determined above, the amount of broadening contributed by hydrodynamic transport through the sample injection channel is calculated to be 18.2%. The amount of broadening contributed by the HDRs and turns is 5.6%. Finally, the majority of the broadening, 76.3%, occurred in the trapezoidal microchannel, which has been shown to yield lower separation efficiencies than round capillaries in previous studies.[70–74] Although turns can cause significant broadening,[75,76] the broadening from the two turns is low in this device, which is likely a result of the turns opposing each other. In addition, the narrow HDR channels between the turns reduce lateral dispersion. Therefore, the initial plug length and broadening associated with the sample extraction are insignificant in the current device.

Simultaneous separation of anions and cations on a PEG coated microfluidic device

Successful injection and separation of anions and cations in different channels are demonstrated using a mixture of model fluorophores, and a mixture consisting of a peptide and proteins. In Fig. 4, representative electropherograms for the separations performed on the microfluidic device are shown and the corresponding average separation efficiencies and standard deviations ($n = 5$) can be found in Table 1. The fluorescent dye mixture analyzed consists of 3 analytes, one cation (R123) and two anions (FLCA and FL). The peptide and protein mixture consists of a TMRIA labeled positive peptide, and FITC labeled BSA, casein, and avidin all of which are negatively charged at the pH used.

Based on the electropherograms shown in Fig. 4, the simultaneous injection and separation of both cations and anions are achieved with suppressed EOF. Furthermore, the suppression of the EOF causes the anions to migrate toward the anode and cations to migrate toward the cathode as expected. Evaluation of the device shows that both cations and anions are extracted and separated in different channels. Furthermore, the anions and cations are only extracted and detected in their respective separation channels as shown in Fig. 4. This lack of cross-detection in the other channel indicates that the bulk flow through

Table 1 The separation efficiencies from the electropherograms shown in Fig. 4–6. The analytes in the table are listed by their elution orders

		Separation efficiency (plates)							
		Dye mixture				Peptide and proteins			
		R123	R123 Neu	FLCA	FL	Pos Pep	Avidin	BSA	Casein
PEG coated microfluidic device	Average	201	—	3,233	3,440	369	897	309	676
	Std. Dev.	19	—	332	392	46	233	165	260
CE separation bare capillary (with EOF)	Average	22,371	31,454	35,082	12,828	74	—	27	18
	Std. Dev.	229	4,491	3,025	1,343	34	—	12	12
CE separation PEG coated capillary (no EOF)	Average	5,630	—	21,159	64,233	1,043	1,870	9,545	13,273
	Std. Dev.	718	—	1,415	10,242	240	358	4,015	1,867

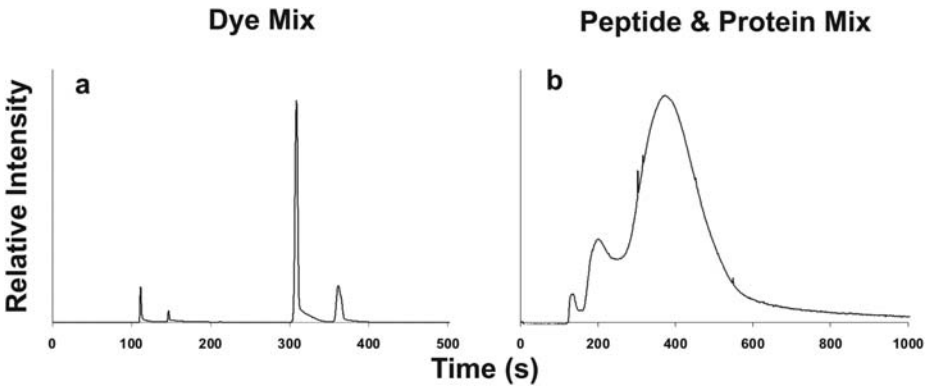

Fig. 5 Representative electropherograms of the separations performed with CE in a bare fused silica capillary with EOF. In (a) the separation of the fluorescent dye mixture, and in (b) the separation of the mixture of peptides and proteins are shown. The dye mixture shows a neutral component from R123 at about 150 s in (a). The neutral component is not observed in Fig. 4a or 6a because it has no charge and EOF is suppressed in the separation presented in Fig. 4a and 6a. A poor separation is achieved with the protein and peptide mixture in the bare fused silica capillary.

electrophoretic channels is suppressed and electrophoresis dominates. Additionally, there is a neutral component of the R123 that is not detected in Fig. 4a, further supporting the suppression of bulk flow in the electrophoretic channels.

The separation of the fluorescent dye mixture in the PEG coated microfluidic device is shown in Fig. 4a. Overall, the separation efficiencies are good with an average efficiency of 201 for the R123 peak and 3,440 for the FL peak (Table 1). The R123 peak width is broader and is tailing, which causes the decreased efficiency. As shown in Table 1, the average separation efficiencies obtained for both of the anionic compounds are greater than 3,000 and the two are baseline resolved even with the short 2 cm channel.

The true utility of the device is shown in Fig. 4b, in which a separation of a cationic peptide and anionic proteins is performed at neutral pH in a single injection. Proteins and peptide are prone to non-specific adsorption and require the use of coatings that reduce non-specific adsorption, and the neutral coating used here also reduces the EOF. The microfluidic device design clearly allows the separation of both anionic and cationic species even when electrophoresis dominates. The separation efficiencies of the proteins and peptide are very good and all are >300 over the short 2 cm separation length. It is likely that less than optimal separation efficiencies are observed due to the roughness of the channels and the trapezoidal channel cross-section because most of the broadening occurs in the electrophoretic separation channel.

Comparison of ME separations with CE

Traditional CE is not capable of simultaneous separation of anions and cations with coatings that suppress EOF. Therefore, a direct comparison between the microfluidic device and CE is not possible, consequently the ME device is compared to CE with both uncoated and PEG coated capillaries. With the uncoated capillaries, EOF is high and simultaneous separation of anions and cations is achieved. With the coated capillaries EOF is substantially reduced and simultaneous separation of anions and cations is not possible; as a result the anions and cations are separated in two different runs with opposite polarity.

Using the bare fused silica capillary, both anions and cations are injected in a single run due to the high EOF produced at pH 7 as typically observed in CE. The electropherogram of the dye components is displayed in Fig. 5a with good separation efficiencies being observed (Table 1). Additionally, significant wall interactions are not observed, although diffusion-limited plug

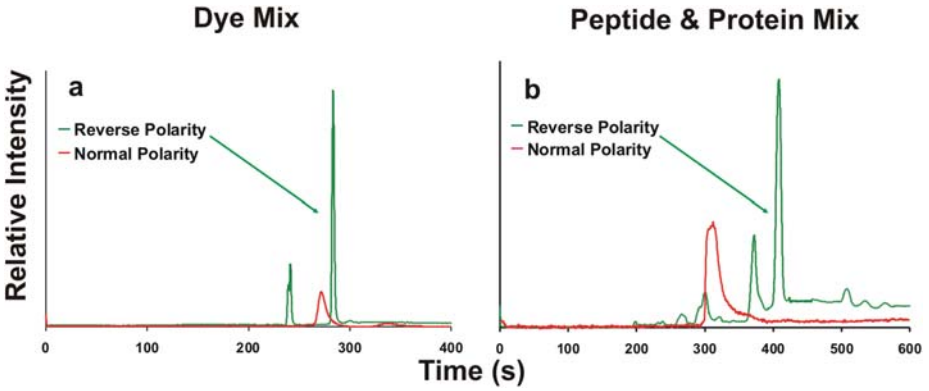

Fig. 6 Representative electropherograms of the separations performed with CE on a PEG coated fused silica capillary with reduced EOF. Two injections using opposite polarities between the separations are required because of the reduced EOF. In (a), the separation of the fluorescent dye mixture is shown, and in (b), the separation of a protein and peptide mixture is shown.

lengths are not achieved. In contrast, the peptide and protein separation on the bare fused silica capillary in Fig. 5b shows substantial broadening leading to an ineffective separation. The highest average separation efficiency was only 74 for the positive peptide, the avidin peak was not observed due to the adsorption, and none of the analytes are baseline resolved. These results clearly indicate that simultaneous separation of proteins and peptides with an uncoated capillary is problematic. The significant adsorption that is observed is somewhat expected because proteins and peptides are well known to experience significant adsorption when separated on bare fused silica capillaries.

A PEG coated capillary was also used to separate the two mixtures with CE. When the CE capillary is coated to reduce non-specific adsorption the EOF is suppressed and two injections are required to separate the anionic and cationic analytes, requiring considerably more time to obtain the electropherograms displayed in Fig. 6. The separation efficiencies are the highest observed as show in Table 1. Probable causes of the improved separation efficiencies are the smooth cylindrical capillary surface and the longer separation length. However, two injections are required that use twice as much sample and the system is difficult to automate and combine with on-line processes or integrate into multidimensional separations.

Experimental determination of the electrophoretic extraction efficiency

Because the amount of sample analyzed directly affects the signal observed, it is crucial to extract as much sample from the hydrodynamic flow as possible. Therefore, the extraction efficiencies are determined for the anions and cations as they pass through the intersection. The experimental values are compared with the theoretical values obtained with a model that we have previously reported and evaluated using only fluorescein.[50] Therefore, this is the first report evaluating the extraction of cations and anions using proteins and peptides.

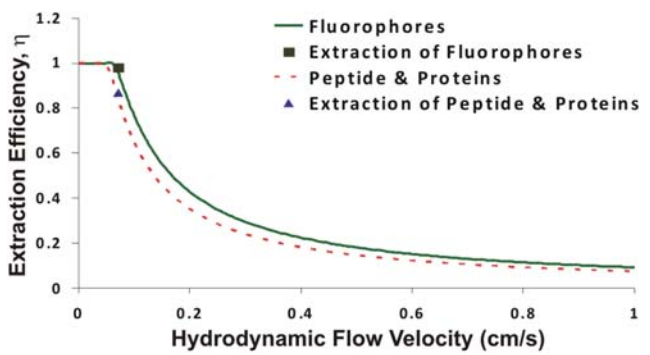

Fig. 7 The extraction efficiency, η, *vs.* the flow velocity. The theoretical curves were generated from the previously reported model and use the weighted average of the electrophoretic velocities of the analytes in the two mixtures. The two data points are the experimentally determined η values calculated from the intensities before and after the sampling intersection. For the dye molecules, η was experimentally measured to be 0.98 and the theoretical value is within 2.6% of the experimental value for the conditions used. For the proteins and peptides, η was experimentally measured to be 0.87 and the theoretical value is within 3.5% of the experimental value.

Using the mathematical model from the previous work, the extraction efficiency was determined from the captured images and found to be 98% for the fluorescent dye mixture and 87% for the peptide and protein mixture. The decreased extraction efficiency for the peptide and protein mixture is a result of the lower electrophoretic mobilities of the analytes compared to the fluorescent dye mixture. Both of the theoretical extraction efficiencies predicted with the model are within 3.5% of the experimental values. The theoretical extraction for each analyte mixture as a function of the hydrodynamic velocity is presented in Fig. 7. In addition, data points corresponding to the experimentally determined extraction efficiency are shown on the graph. The theoretical extraction curve shown in Fig. 7 is based on the weighted average of the electrophoretic mobilities of the analytes in the mixtures.

Conclusions

The work performed here shows the ability to extract charged analyte from a hydrodynamic flow stream and rapidly and simultaneously separates both cations and anions on a PEG coated microfluidic device with suppressed EOF. The analytes are injected from a central sample introduction channel, through which the solution is driven hydrodynamically. The PEG coating reduces protein and peptide adsorption and the simultaneous separation of anionic proteins and a cationic peptide is demonstrated. The HDRs and PEG coating reduce the bulk flow in the electrophoretic separation channels to negligible levels, which allows the anions and cations to only be extracted into their corresponding electrophoretic separation channel. The method used here also removes the separation bias encountered in separations that utilize EOF. In addition, the microchannel design provides simultaneous detection of cations and anions without the possibility of co-detection associated with DOI-CE and elution into different reservoirs.

The use of the unique sampling intersection in this device, previously modeled, enabled the calculation of the extraction efficiency of the analytes being investigated. The predicted extraction efficiencies calculated from the mathematical model for the two samples agreed within 3.5% of experimental values. Finally, the sampling intersection featured here could find further use in creating a 2D LC-CE separation that can, if desired, extract nearly 100% of charged analyte from the effluent of an HPLC separation and subject it to an additional electrophoretic separation.

Acknowledgements

This work is funded in part through NSF RII award EPS 0554328, for which the WV EPSCoR Office and the WVU Research Corp provided matching funds.

References

1 M. Mohamadi, N. Kaji, M. Tokeshi and Y. Baba, *Anal. Chem.*, 2007, **79**, 3667–3672.
2 S. M. Kim, M. A. Burns and E. F. Hasselbrink, *Anal. Chem.*, 2006, **78**, 4779–4785.
3 G. Proczek, V. Augustin, S. Descroix and M.-C. Hennion, *Electrophoresis*, 2009, **30**, 515–524.

4 Z. Long, D. Liu, N. Ye, J. Qin and B. Lin, *Electrophoresis*, 2006, **27**, 4927–4934.
5 B. Jung, R. Bharadwaj and J. G. Santiago, *Electrophoresis*, 2003, **24**, 3476–3483.
6 Z. Long, Z. Shen, D. Wu, J. Qin and B. Lin, *Lab Chip*, 2007, **7**, 1819–1824.
7 J. D. Ramsey and G. E. Collins, *Anal. Chem.*, 2005, **77**, 6664–6670.
8 A. V. Hatch, A. E. Herr, D. J. Throckmorton, J. S. Brennan and A. K. Singh, *Anal. Chem.*, 2006, **78**, 4976–4984.
9 M. Ghitun, E. Bonneil, M.-H. Fortier, H. Yin, K. Killeen and P. Thibault, *J. Sep. Sci.*, 2006, **29**, 1539–1549.
10 A. B. Jemere, R. D. Oleschuk, F. Ouchen, F. Fajuyigbe and D. J. Harrison, *Electrophoresis*, 2002, **23**, 3537–3544.
11 B. Y. Kim, J. Yang, M. Gong, B. R. Flachsbart, M. A. Shannon, P. W. Bohn and J. V. Sweedler, *Anal. Chem.*, 2009, **81**, 2715–2722.
12 Y. Cong, L. Zhang, D. Tao, Y. Liang, W. Zhang and Y. Zhang, *J. Sep. Sci.*, 2008, **31**, 588–594.
13 J. D. Ramsey, S. C. Jacobson, C. T. Culbertson and J. M. Ramsey, *Anal. Chem.*, 2003, **75**, 3758–3764.
14 *Biological Applications of Microfluidics*, ed. F. A. Gomez, John Wiley & Sons, Inc., Hoboken, 2008.
15 D. C. Liebler, in *Introduction to Proteomics Tools for the New Biology*, ed. Kim Hoather-Potter, Humana Press Inc., Totowa, NJ, 2002.
16 J. V. Olsen, B. Blagoev, F. Gnad, B. Macek, C. Kumar, P. Mortensen and M. Mann, *Cell*, 2006, **127**, 635–648.
17 E. M. Pasini, M. Kirkegaard, P. Mortensen, H. U. Lutz, A. W. Thomas and M. Mann, *Blood*, 2006, **108**, 791–801.
18 A. Motoyama, J. D. Venable, C. I. Ruse and J. R. Yates, III, *Anal. Chem.*, 2006, **78**, 5109–5118.
19 F. Forner, L. J. Foster, S. Campanaro, G. Valle and M. Mann, *Mol. Cell. Proteomics*, 2006, **5**, 608–619.
20 E. I. Chen, J. Hewel, B. Felding-Habermann and J. R. Yates, III, *Mol. Cell. Proteomics*, 2006, **5**, 53–56.
21 Y. Shen, R. Zhang, R. J. Moore, J. Kim, T. O. Metz, K. K. Hixson, R. Zhao, E. A. Livesay, H. R. Udseth and R. D. Smith, *Anal. Chem.*, 2005, **77**, 3090–3100.
22 L. Wu and D. K. Han, *Expert Rev. Proteomics*, 2006, **3**, 611–619.
23 D. A. Egas and M. J. Wirth, *Annu. Rev. Anal. Chem.*, 2008, **1**, 833–855.
24 M. J. Wirth, *Anal. Chem.*, 2007, **79**, 800–808.
25 J. H. Wahl, D. C. Gale and R. D. Smith, *J. Chromatogr., A*, 1994, **659**, 217–222.
26 J. H. Wahl, D. R. Goodlett, H. R. Udseth and R. D. Smith, *Electrophoresis*, 1993, **14**, 448–457.
27 M. A. Moseley, J. W. Jorgenson, J. Shabanowitz, D. F. Hunt and K. B. Tomer, *J. Am. Soc. Mass Spectrom.*, 1992, **3**, 289–300.
28 D. C. Simpson and R. D. Smith, *Electrophoresis*, 2005, **26**, 1291–1305.
29 K. D. Lukacs, PhD thesis, The University of North Carolina, 1983.
30 M. Moini and H. Huang, *Electrophoresis*, 2004, **25**, 1981–1987.
31 E. Schiffer, H. Mischak and J. Novak, *Proteomics*, 2006, **6**, 5615–5627.
32 B. S. Weekley and J. P. Foley, *Electrophoresis*, 2007, **28**, 697–711.
33 E. Ostuni, R. G. Chapman, R. E. Holmlin, S. Takayama and G. M. Whitesides, *Langmuir*, 2001, **17**, 5605–5620.
34 T. T. Razunguzwa, M. Warrier and A. T. Timperman, *Anal. Chem.*, 2006, **78**, 4326–4333.
35 J. Liu, T. Pan, A. T. Woolley and M. L. Lee, *Anal. Chem.*, 2004, **76**, 6948–6955.
36 K. Uchida, H. Otsuka, M. Kaneko, K. Kataoka and Y. Nagasaki, *Anal. Chem.*, 2005, **77**, 1075–1080.
37 H. Bi, S. Meng, Y. Li, K. Guo, Y. Chen, J. Kong, P. Yang, W. Zhong and B. Liu, *Lab Chip*, 2006, **6**, 769–775.
38 S. Lee and J. Voros, *Langmuir*, 2005, **21**, 11957–11962.
39 A. Padarauskas, *Curr. Anal. Chem.*, 2005, **1**, 149–156.
40 D. Durkin and J. P. Foley, *Electrophoresis*, 2000, **21**, 1997–2009.
41 A. Padarauskas, *Rev. Anal. Chem.*, 2001, **20**, 271–301.
42 C. Johns, W. Yang, M. Macka and P. R. Haddad, *J. Chromatogr., A*, 2004, **1050**, 217–222.
43 C. M. White, R. Luo, S. A. Archer-Hartmann and L. A. Holland, *Electrophoresis*, 2007, **28**, 3049–3055.
44 P. Kuban and B. Karlberg, *Anal. Chem.*, 1998, **70**, 360–365.
45 A. Padarauskas, V. Olsauskaite and G. Schwedt, *J. Chromatogr., A*, 1998, **800**, 369–375.
46 F. Priego-Capote and M. D. Luque de Castro, *Electrophoresis*, 2005, **26**, 2283–2292.
47 M. X. Zhou and J. P. Foley, *Electrophoresis*, 2004, **25**, 653–663.
48 F. Priego-Capote and M. D. Luque de Castro, *Electrophoresis*, 2004, **25**, 4074–4085.
49 J. Wang, G. Chen, A. Muck, Jr and G. E. Collins, *Electrophoresis*, 2003, **24**, 3728–3734.
50 B. R. Reschke, H. Luo, J. Schiffbauer, B. F. Edwards and A. T. Timperman, *Lab Chip*, 2009, **9**, 2203–2211.
51 T. T. Razunguzwa, J. Lenke and A. T. Timperman, *Lab Chip*, 2005, **5**, 851–855.
52 T. T. Razunguzwa and A. T. Timperman, *Anal. Chem.*, 2004, **76**, 1336–1341.
53 C. S. Eftenhauser, A. Manz and H. M. Wldmer, *Anal. Chem. (Washington, DC, U. S.)*, 1995, **67**, 2284–2287.
54 S. C. Jacobson, C. T. Culbertson, J. E. Daler and J. M. Ramsey, *Anal. Chem. (Washington, DC, U. S.)*, 1998, **70**, 3476–3480.
55 J. P. Alarie, S. C. Jacobson and J. M. Ramsey, *Electrophoresis*, 2001, **22**, 312–317.
56 J. P. Alarie, S. C. Jacobson, C. T. Culbertson and J. M. Ramsey, *Electrophoresis*, 2000, **21**, 100–106.
57 S. Liu, Y. Shi, W. W. Ja and R. A. Mathies, *Anal. Chem. (Washington, DC, U. S.)*, 1999, **71**, 566–573.
58 Y. Shi, P. C. Simpson, J. R. Scherer, D. Wexler, C. Skibola, M. T. Smith and R. A. Mathies, *Anal. Chem. (Washington, DC, U. S.)*, 1999, **71**, 5354–5361.
59 L. D. Hutt, D. P. Glavin, J. L. Bada and R. A. Mathies, *Anal. Chem. (Washington, DC, U. S.)*, 1999, **71**, 4000–4006.
60 G. Ocvirk, M. Munroe, T. Tang, R. Oleschuk, K. Westra and D. J. Harrison, *Electrophoresis*, 2000, **21**, 107–115.
61 A. Ramseier, J. Caslavska and W. Thormann, *Electrophoresis*, 1998, **19**, 2956–2966.
62 J. P. Kutter, S. C. Jacobson, N. Matsubara and J. M. Ramsey, *Anal. Chem. (Washington, DC, U. S.)*, 1998, **70**, 3291–3297.
63 A. G. Hadd, S. C. Jacobson and J. M. Ramsey, *Anal. Chem. (Washington, DC, U. S.)*, 1999, **71**, 5206–5212.
64 Y. Liu, R. S. Foote, S. C. Jacobson, R. S. Ramsey and J. M. Ramsey, *Anal. Chem. (Washington, DC, U. S.)*, 2000, **72**, 4608–4613.
65 S. C. Jacobson, L. B. Koutny, R. Hergenroder, A. W. Moore and J. M. Ramsey, *Anal. Chem. (Washington, DC, U. S.)*, 1994, **66**, 3472–3476.
66 T. F. Hooker and J. W. Jorgenson, *Anal. Chem.*, 1997, **69**, 4134–4142.
67 A. V. Lemmo and J. W. Jorgenson, *Anal. Chem.*, 1993, **65**, 1576–1581.
68 J. C. Giddings, in *Unified Separation Science*, John Wiley & Sons, Inc., New York, 1991, pp. 58–61.
69 A. Weston and P. R. Brown, *HPLC and CE Principles and Practice*, Academic Press, San Diego, 1997.
70 Y. Xu, S. Chen, X. Feng, W. Du, Q. Luo and B.-F. Liu, *Electrophoresis*, 2008, **29**, 734–739.
71 A. Cifuentes and H. Poppe, *Chromatographia*, 1994, **39**, 391–404.
72 A. Cifuentes, M. A. Rodrfguez and F. J. Garcia-Montelongo, *J. Chromatogr., A*, 1996, **737**, 243–253.
73 S. K. Griffiths and R. H. Nilson, *Anal. Chem.*, 2000, **72**, 4767–4777.
74 X. Zhang and F. E. Regnier, *J. Chromatogr., A*, 2000, **869**, 319–328.
75 C. T. Culbertson, S. C. Jacobson and J. M. Ramsey, *Anal. Chem.*, 1998, **70**, 3781–3789.
76 J. I. Molho, A. E. Herr, B. P. Mosier, J. G. Santiago, T. W. Kenny, R. A. Brennen, G. B. Gordon and B. Mohammadi, *Anal. Chem.*, 2001, **73**, 1350–1360.